

DESIGNING A SEQUENTIAL-MODULAR STEADY-STATE SIMULATOR FOR KRAFT RECOVERY CYCLE EVAPORATIVE SYSTEMS

Authors: Márcio R. Vianna Neto^{1,2}, Marcelo Cardoso¹, Ekaterina Sermyagina², Esa K. Vakkilainen², Eder D. Oliveira¹

¹ Federal University of Minas Gerais (UFMG). Brazil

² Lappeenranta-Lahti University of Technology LUT. Finland

ABSTRACT

A sequential-modular process simulator was developed for simulating Kraft recovery cycle evaporation plants under steady-state conditions. The simulation engine was written in C++ and has been made freely available to the scientific and technical communities. The engine included subroutines for ordering, partitioning, and tearing flowsheets, as well as for converging torn flowsheet streams. In this paper, these core subroutines are described. Evaporator calculations are based on steam table correlations and black liquor enthalpy correlations described in literature. The numerical method used for converging torn streams in this implementation was the well-known Wegstein Method. Five multiple-effect counter-current evaporator scenarios, ranging from 3 to 7 effects, were used to profile the simulator. The simulator was shown to be robust enough to be used for simulating evaporator arrangements that are typically found in the pulp and paper industry. The robustness of convergence found in the tested scenarios suggests that the simulator could be extended to accommodate more complex systems. The simulator converged quickly to all solutions, suggesting that it may be used for performing optimization of evaporative systems.

Keywords: simulator, steady state, evaporator, black liquor, sequential-modular

INTRODUCTION

As the Pulp and Paper industry strives to attenuate its environmental impact by reducing carbon dioxide emissions, while still maintaining a competitive edge, it becomes ever-more important to develop process optimization techniques that can account for all these factors. Process optimization techniques assume that a reliable model for the process being studied is available, and these models are commonly built using process simulation software known as process simulators. Better process simulators allow a wider range of optimization scenarios to be considered and yield more accurate calculation results.

The energetic optimization of chemical pulping plants has recently received attention in the literature [1,2] because increasing its energetic efficiency contributes both to the overall process competitiveness and to the reduction of fossil-fueled carbon dioxide generation, as less energy resources will be demanded by the process. The latter contribution is key to achieving sustainable development [3,4].

A fundamental process in chemical pulping plants is black liquor evaporation. Black liquor is a residue produced during this process. In the chemical recovery cycle, black liquor is burned in the recovery boiler to produce energy and to recover chemicals that are consumed during the cooking step. An effective black liquor burning strongly contributes to making the chemical pulping process economically feasible [2, 5–7].

To ensure that the black liquor is effectively burned in the recovery boiler and to increase the liquor combustion efficiency, its water fraction must be increased. Evaporation and drying are the most energy-intensive steps in the chemical pulping process. Evaporation is typically carried out in a multiple-effect evaporator (MEE) train, usually constituted of 5 to 7+ evaporator bodies. MEE trains concentrate black liquors from a dry solids mass fraction of approximately 15% to about 80–85% [8]. The evaporation step accounts for 24–30% of the total energy consumed by a pulp mill, which makes the optimization of this step an important goal [9].

MEE optimization can be exceptionally complex because the set of possible evaporator body arrangements may be very large, each of which having different thermodynamic characteristics. For this reason, until recently, evaporator system optimization methodologies described in literature required the user to pre-select the arrangements to be considered during optimization and hard code them. This process is tedious and error prone. Recently, Verma *et al.* (2019) published a comprehensive review of methods used for modeling and optimizing evaporator trains [12]. Deterministic and stochastic nonlinear programming

Corresponding author: Vianna Neto, M. R. Lappeenranta-Lahti University of Technology / Federal University of Minas Gerais (UFMG). Av. Pres. Antônio Carlos, 6627 – Pampulha. Belo Horizonte – MG – Brazil - 31270-901. Phone: +55-31-34091735
Email: marciorneto@ufmg.br

techniques have also been used to optimize the energy consumption in preexisting evaporator plants [10–14].

Vianna Neto et al. (2020) presented a methodology that allowed several structural MEE arrangements to be considered without having to hard code them individually [15]. Using this methodology, the authors successfully optimized a small 3-effect scenario and a realistic 6-effect system. This methodology used in its core an equation-oriented steady-state MEE simulator [16].

In this paper, we modify the equation-oriented simulator developed by Vianna Neto et al. (2020) to a sequential-modular design. The new design has very good convergence properties and naturally allows for evaporators operating under non-equilibrium conditions to be simulated. The simulator converged quickly and reliably, suggesting that it can be used for evaporator systems optimization.

METHODS

Simulator architecture

The new simulator design follows a sequential-modular approach (SMA), which means that each unit operation being simulated is abstracted as a module that is calculated independently from all the others. A graphical user interface (GUI) is exposed, through which it is possible to assemble the block diagram corresponding to the MEE system under study and to input process parameters. In these diagrams, unit processes are represented as blocks, which are interconnected through streams.

In SMA simulators, the process blocks calculation order is heavily influenced by the process flowsheet. Figure 1 represents a system of 3 process modules, here represented by rectangular blocks, and 6 streams, represented by arrows. In this example, each module is connected to 2 input streams and 2 output streams.

If the properties of the leftmost process streams are known, module 1 can be executed to calculate the properties of its two output streams. These streams serve as input to module 2. Since their properties are now known, module 2 can be calculated to determine its outlet streams. These, in turn, serve as inputs to module 3. Upon calculating module 3, the rightmost streams can finally be obtained. The properties of all streams can thus be determined by executing the modules in a certain order, in this example, 1-2-3.

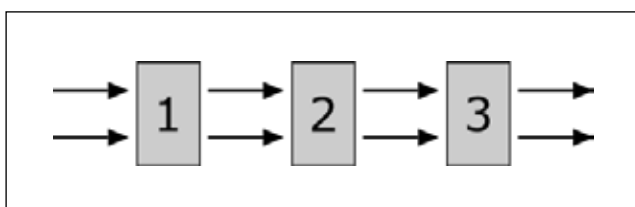


Figure 1. Calculation of a process model using a SMA methodology. The process topology suggests that the modules should be calculated in the order 1-2-3

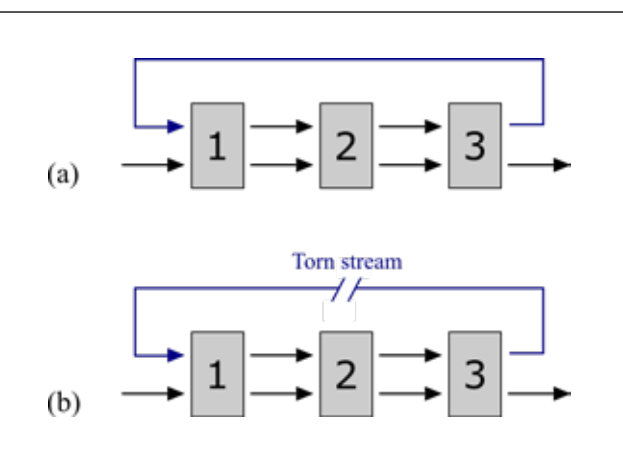


Figure 2. Stream tearing procedure in a SMA simulator

In practical systems, however, it is very common to find topologies such as the one shown in Figure 2a, where the blue stream serves as input to module 1 and as output to module 3. This topological feature is commonly known as a recycle, for which reason the blue stream is referred to as a recycle stream. In this case, the calculation is not as straightforward as before since the calculation of module 1 requires information that can only be obtained by calculation module 3. Module 3, on the other hand, depends on the outputs of module 1. In MEE systems, counter-current liquor-vapor arrangements are common, and cause recycles to exist.

In the presence of recycles, an iterative procedure must be carried out. In Figure 2b, the recycle stream has been torn. In the procedure known as stream tearing, recycles are eliminated by breaking recycle streams into pairs of independent streams [17, 18]. The calculation sequence, in this example, begins with an initial estimate for the properties of the torn stream. Given this initial guess, module 1 can be executed, followed by modules 2 and 3. The result from module 3 will yield new property values for the torn stream which will, in general, be different than the initial estimate. Based on these new values, the torn stream properties can be updated. This process is repeated until the difference is sufficiently small. This procedure is sometimes referred to as converging the recycles.

In this work, the simulator selected the tear streams based on the number of recycles that their tearing would remove. Streams that caused the most loops to be removed were given higher priority and the procedure was carried out until no recycles remained. Several numerical procedures for recycle convergence are available, such as fixed-point iteration, Wegstein method and the Newton-Raphson method [19]. In this paper, we compare the performance of two schemes: fixed-point iteration and Wegstein method.

The GUI was developed using Python 3.8, whereas the stream tearing algorithms, as well as the numerical routines were implemented in C++.

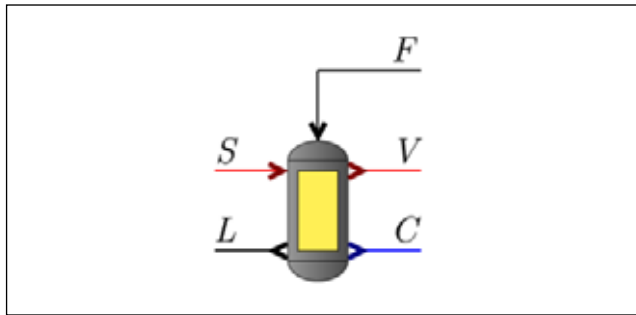


Figure 3. Evaporator block as represented in the SMA simulator

Evaporator and stream models

The GUI block representation for evaporators is shown in Figure 3. Evaporator blocks accept as inputs a black liquor stream F and a vapor stream S. Its outlets are a concentrated black liquor stream L, a condensate stream C and a vapor stream V.

The evaporator model solves equations 1 through 10 using the Newton-Raphson method. In these equations, variable subscripts denote the streams to which they correspond, except the subscript sat, which denotes saturation. Mass flows are indicated by , enthalpies by H, temperatures and pressures by T and P respectively, the dissolved solids mass fraction by x_D , and the boiling point rise of black liquor, by BPR.

$$\dot{m}_S = \dot{m}_C \quad (1)$$

$$\dot{m}_F = \dot{m}_L + \dot{m}_V \quad (2)$$

$$\dot{m}_F x_{D,F} = \dot{m}_L x_{D,L} \quad (3)$$

$$P_S = P_C \quad (4)$$

$$T_C = T_{sat}(P_S) \quad (5)$$

$$T_V = T_{sat}(P_V) + BPR(P_V, x_{D,L}) \quad (6)$$

$$T_V = T_L \quad (7)$$

$$Q = \dot{m}_S (H_S - H_C) \quad (8)$$

$$Q = UA(T_S - T_L) \quad (9)$$

$$Q + \dot{m}_F H_F = \dot{m}_L H_L + \dot{m}_V H_V \quad (10)$$

Table 2. Stream types and their describing variables.

Stream type	Variables
Black liquor	\dot{m}, T, x_D
Vapor and condensate	\dot{m}, T, P, H, x_v

Evaporator blocks also take as user set parameters the heat transfer coefficient U and the heat transfer area A. Table 2 lists the variables describing each type of stream, where denotes vapor quality.

Physical properties

Physical properties were estimated following the methodology described by Vianna Neto et al. (2020) [15]. Water and steam enthalpies were calculated from steam table correlations, implemented in C++ as described in the 2007 revised release on the IAPWS Industrial Formulation of 1997 standard [20].

Black liquor enthalpies were calculated from the correlation described by Zaman and Fricke (1996), which expresses the enthalpy of black liquor at 80°C, H_{80} , as shown in Equation (11) [21]. In this equation, H_w denotes the water enthalpy at 80°C, x_D is the black liquor dissolved solids fraction, and the constants and depend on the type of black liquor being considered. In this work, it was assumed that $b = 105.0 \text{ kJ/kg.K}$ and $c = 0.300$.

$$H_{80} = H_w + b \left[-1 + \exp \left(\frac{x_D}{c} \right) \right] \quad (11)$$

To account for black liquor enthalpies at other temperatures, H_{80} is corrected using the black liquor specific heat correlation given by Equation (12) [5]

$$c_p = 4.216(1-x_D) + \left[1.675 + \frac{3.31t}{1000.0} \right] x_D + \left[4.87 + \frac{20t}{1000.0} \right] (1-x_D)x_D^3 \quad (12)$$

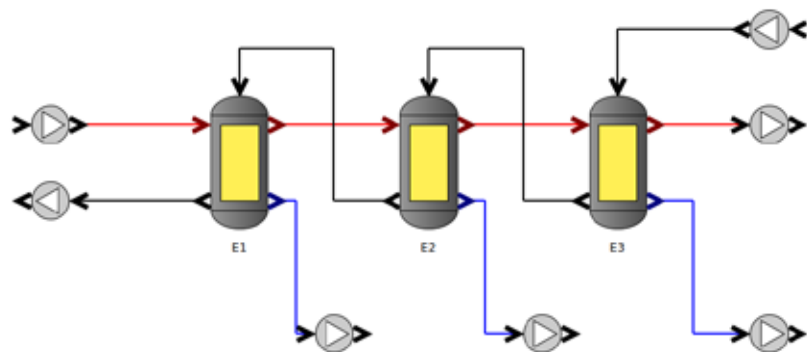
The black liquor boiling point rise (BPR) also needs to be considered in evaporator calculations. BPR is accounted for using Equations (13) and (14).

$$BPR(P, x_D) = BPR_{atm}(x_D)[1 + 0.6(T_P - 373.16)/100] \quad (13)$$

$$BPR_{atm}(x_D) = 6.173x_D^7 - 7.48x_D^5 + 32.747x_D^3 \quad (14)$$

Table 3. Input values for the tested MEE systems.

Variable	Value(s)	Units
Live steam temperature	120	°C
Live steam mass flow	0.0, 2.5 and 5.0	kg/s
Black liquor inlet mass flow	50	kg/s
Black liquor inlet temperature	70	°C
Black liquor inlet dissolved solids	20	%
Vapor temperature from Effect 3	60	°C
Heat transfer coefficient of all effects (U)	1.2	kW/m ² K
Heat transfer area of all effects (A)	1040	m ²

**Figure 4.** Simple 3-effect MEE system, adapted from [5]. Larger systems follow this same general counter-current structure

Test scenarios

A simple 3-effect system, shown in Figure 4, based on the scenario described in Tikka, 2008, was used as the base for building all test scenarios [5]. MEE systems ranging from 3 to 7 evaporator bodies were constructed, while maintaining the same counter-current structure shown in Figure 4. The systems were initially simulated for three values of live steam mass flow: 0, 2.5 and 5.0 kg/s. This first step was meant to assess how well the simulator could calculate scenarios where evaporation would not necessarily occur due to a low supply of steam. The number of iterations to convergence for each test was recorded. Table 3 lists the input values used for all tested scenarios.

Each system was then simulated 100 times, with a fixed live steam mass flow of 5.0 kg/s, to measure the computational time required for the simulation to finish. This result is of great practical importance because the convergence time directly affects how practical it will be in optimization studies. The computer where all simulations were executed was equipped with a 2.7 GHz Intel® Core™ i7 and 4GB RAM, and was run on Ubuntu 16.04.

RESULTS AND DISCUSSION

Figure 5 shows the number of iterations required for each system to converge for different live steam mass flows. The number of iterations ranged from 10, for the 3-effect system, to almost 100, for the 7-effect system. The simulator behaved very reliably, converging for all scenarios. It is worth mentioning that the simulator converged well without having to resort to simplified models as was done originally by Vianna Neto et al. (2020) [16].

The number of iterations increases as the systems grow larger. This is to be expected, because larger systems require more recycles to be torn and, therefore, more convergence variables to converge. The number of iterations grows as live steam mass flow approaches 0. When steam mass flow values are low, evaporator modules alternate between letting off steam and not evaporating at all as the iterations proceed. This switching behavior slows convergence and causes the number of iterations to increase.

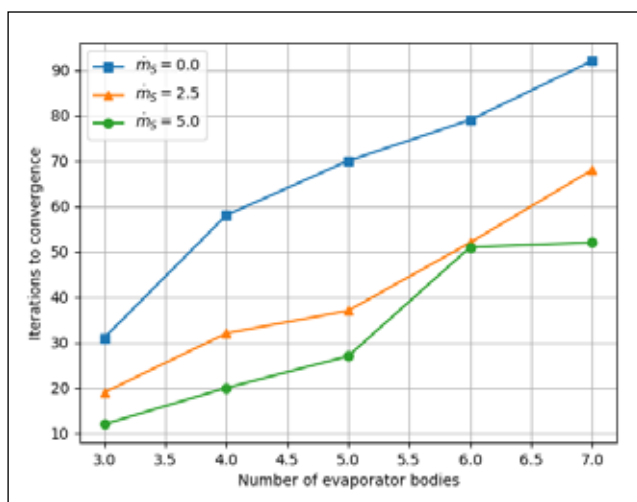


Figure 5. Number of iterations required for each system to converge

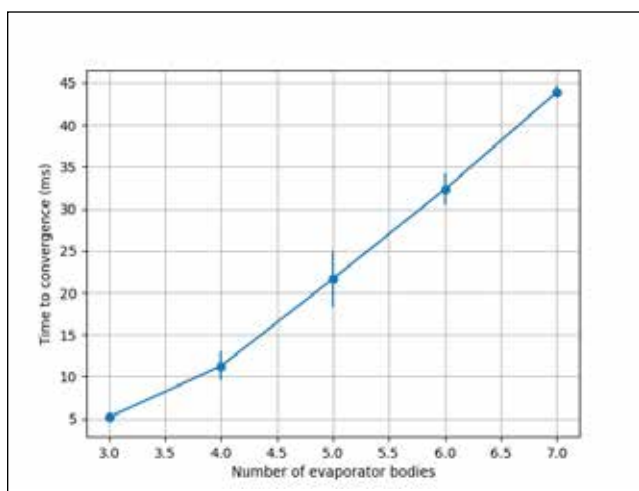


Figure 6. Mean computational time in milliseconds required for each system to converge over 100 runs. Vertical bars denote standard deviations

Figure 6 shows the mean computational time in milliseconds required for each system to converge over 100 runs. The vertical bars shown in the figure represent standard deviations. Notice that running times range from 5 to 50ms, thus allowing it to be used alongside with optimization algorithms. Standard deviations are relatively small, on the order of 5ms, being most noticeable in the 5-effect scenarios. As would be expected, running times increase as the systems grow larger. This is a direct consequence of larger iteration numbers to converge.

4. CONCLUSIONS

The simulator displayed very good convergence properties and proved to be reliable for calculating realistic-sized MEE systems. It also converges quickly, which suggests that it may be used for performing evaporator systems optimization, possibly with the use of stochastic algorithms, which require the systems to be calculated several times.

The simulator currently assumes that the heat transfer coefficient is provided by the user. In practice, however, it would be desirable to automatically calculate these coefficients using heat transfer correlations, as they are dependent on evaporator operating conditions. Naturally, the simulator should be extended to accommodate other recovery cycle unit processes, such as flash drums, preheaters, and recovery boilers. It is also important that different MEE topologies be tested to check if the good convergence behavior verified in this study holds for systems of arbitrary structure.

ACKNOWLEDGEMENTS

This study was done in the frames of the project “Role of forest industry transformation in energy efficiency improvement and reducing CO₂ emissions” funded by Academy of Finland. The authors are also indebted to the Conselho Nacional de Desenvolvimento Científico e Tecnológico (CNPq/BRAZIL) and Fundação de Amparo à Pesquisa do Estado de Minas Gerais (Fapemig/BRAZIL) for supporting this study. ■

REFERENCES

1. S. Mesfun and A. Toffolo, “Optimization of process integration in a Kraft pulp and paper mill–Evaporation train and CHP system,” *Applied energy*, vol. 107, pp. 98–110, 2013.
2. X. Ji, J. Lundgren, C. Wang, J. Dahl, and C.-E. Grip, “Simulation and energy optimization of a pulp and paper mill–Evaporation plant and digester,” *Applied energy*, vol. 97, pp. 30–37, 2012.
3. T. Fleiter, D. Fehrenbach, E. Worrell, and W. Eichhammer, “Energy efficiency in the German pulp and paper industry–A model-based assessment of saving potentials,” *Energy*, vol. 40, no. 1, pp. 84–99, 2012.
4. L. Kong, A. Hasanbeigi, and L. Price, “Assessment of emerging energy-efficiency technologies for the pulp and paper industry: a technical review,” *Journal of Cleaner Production*, vol. 122, pp. 5–28, 2016.

REFERENCES

5. P. Tikka, "Chemical pulping part 2, Recovery of chemicals and energy," *Papermaking Science and Technology*, 2008.
6. M. Cardoso, K. D. de Oliveira, G. A. A. Costa, and M. L. Passos, "Chemical process simulation for minimizing energy consumption in pulp mills," *Applied Energy*, vol. 86, no. 1, pp. 45–51, 2009.
7. D. M. Saturnino, Modeling of kraft mill chemical balance. PhD thesis, University of Toronto, 2012.
8. M. R. Olsson, Simulations of Evaporation Plants in Kraft Pulp Mills: Including Lignin Extraction and Use of Excess Heat. PhD thesis, Chalmers University of Technology, 2009.
9. G. Jyoti and S. Khanam, "Simulation of heat integrated multiple effect evaporator system," *International Journal of Thermal Sciences*, vol. 76, pp. 110–117, 2014.
10. O. P. Verma, G. Manik, V. K. Jain, D. K. Jain, H. Wang, et al., "Minimization of energy consumption in multiple stage evaporator using genetic algorithm," *Sustainable Computing: Informatics and Systems*, vol. 20, pp. 130–140. (2018).
11. O. P. Verma, T. H. Mohammed, S. Mangal, and G. Manik, "Minimization of energy consumption in multi-stage evaporator system of kraft recovery process using interior-point method," *Energy*, vol. 129, pp. 148–157. (2017).
12. O. P. Verma, G. Manik, and S. K. Sethi, "A comprehensive review of renewable energy source on energy optimization of black liquor in MSE using steady and dynamic state modeling, simulation and control," *Renewable and Sustainable Energy Reviews*, vol. 100, pp. 90–109. (2019).
13. M. Khademi, M. Rahimpour, and A. Jahanmiri, "Simulation and optimization of a six-effect evaporator in a desalination process," *Chemical Engineering and Processing: Process Intensification*, vol. 48, no. 1, pp. 339–347. (2009).
14. D. Srivastava, B. Mohanty, and R. Bhargava, "Modeling and simulation of mee system used in the sugar industry," *Chemical engineering communications*, vol. 200, no. 8, pp. 1089–1101. (2013). 22. S. Khanam and B. Mohanty, "Energy reduction schemes for multiple effect evaporator systems," *Applied Energy*, vol. 87, no. 4, pp. 1102– 1111. (2010).
15. Vianna Neto, M. R, Saari, J., Vakkilainen, E. K., Cardoso, M.and Oliveira, E. D., "A superstructure-based methodology for simultaneously sizing and arranging additional evaporator bodies in multiple-effect evaporator plants", *Journal of Science & Technology for Forest Products and Processes*, vol. 7, no. 6, pp. 36-47, 2020.
16. Vianna Neto, M.R., Cardoso, M., Vakkilainen, E. K. and Oliveira, E. D., "Development of an equation-oriented steady-state evaporation plant simulator", *O Papel*, vol. 81, no. 7, pp. 83-89, 2020.
17. R. S. H. Mah, "Chemical process structures and information flows", Elsevier, 2013.
18. A. W. Westerberg, "Process flowsheeting", Cambridge University Press, 1979.
19. R. Smith, "Chemical process: design and integration", John Wiley & Sons, 2005.
20. W. Wagner and H.-J. Kretzschmar, *International Steam Tables-Properties of Water and Steam based on the Industrial Formulation IAPWSIF97: Tables, Algorithms, Diagrams, and CD-ROM Electronic Steam Tables-All of the equations of IAPWS-IF97 including a complete set of supplementary backward equations for fast calculations of heat cycles, boilers, and steam turbines*. Springer Science & Business Media. (2007).
21. A. Zaman and A. Fricke, "Heat of dilution and enthalpy concentration relations for slash pine kraft black liquors," *Chemical Engineering Communications*, vol. 155, no. 1, pp. 197–216. (1996).